Open Access Indonesian Journal of Medical Reviews
Volume 6, Issue 5, 2026 | Article ID: 943 | Pages: 470–482 | e-ISSN 2807-6257
OAIJMR

CASE STUDY

Multimodal Imaging and Longitudinal Trajectory Analysis of Recurrent Ocular Toxoplasmosis and Contralateral Early-Onset Cataract: An Observational Analytic Case Study

Iska Novi Udayani[1], Daniel Johosua Siegers[2*], I Gusti Ayu Made Juliari[3], I Wayan Ardy Paribrajaka[2]

[1] Ophthalmology Residency Program, Faculty of Medicine, Universitas Udayana, Denpasar, Indonesia
[2] Ophthalmologist, Ambon-Vlissingen Eye Clinic, Ambon, Indonesia
[3] Ocular Infection and Immunology Division, Ophthalmology Department, Faculty of Medicine, Universitas Udayana, Denpasar, Indonesia

ARTICLE INFO

Article history
Received: July 30, 2026
Revised: August 27, 2026
Accepted: September 18, 2026
Available Online: September 23, 2026
Published: September 29, 2026

Keywords
Early-onset cataract; Multimodal imaging; Observational analytic case study; Ocular toxoplasmosis; Retinochoroiditis; Toxoplasma gondii

***Corresponding author**
Daniel Johosua Siegers
E-mail: Siegersdaniel@yahoo.com

DOI
https://doi.org/10.37275/oaijmr.v6i5.943

ABSTRACT

Background: Ocular toxoplasmosis is the leading cause of infectious posterior uveitis. A dense cataract in an otherwise quiet fellow eye creates a clinical dilemma between bilateral parasitic dissemination and an independent coexisting disorder.

Objective: To characterize the longitudinal structural and functional trajectories of recurrent ocular toxoplasmosis with contralateral early-onset cataract and to assess whether the two conditions were causally related.

Methods: This ethically approved longitudinal observational analytic case study followed a 37-year-old woman from baseline to week 6. Assessments included visual acuity, tonometry, B-scan ultrasonography, fundus photography, spectral-domain optical coherence tomography, and serological assays.

Result: At baseline, right-eye vision was light perception because of an isolated mature grade 4 cataract without signs of uveitis, whereas the left eye had 6/18 vision with active juxtafoveal retinochoroiditis and a peripapillary scar. Anti-Toxoplasma gondii IgG was reactive (393.4 IU/mL) and IgM was nonreactive. After phacoemulsification and intraocular lens implantation, right-eye visual acuity reached 6/6 by postoperative day 3, and imaging revealed a pristine neuroretina with a central macular thickness of 219 μm. Oral trimethoprim-sulfamethoxazole followed by tapered methylprednisolone consolidated the left retinochoroidal lesion and restored 6/6 vision by week 6.

Conclusion: Marked interocular asymmetry in ocular toxoplasmosis requires multimodal structural verification. In this patient, the contralateral early-onset cataract represented independent coexistence rather than bilateral parasitic causality.

1. Introduction

Toxoplasma gondii is an obligate intracellular protozoan parasite of the phylum Apicomplexa that maintains a ubiquitous global distribution and demonstrates an exceptional capacity to establish lifelong chronic infection within human neural and ocular tissues.[1] Systematic epidemiological assessments estimate that approximately one-third of the global human population harbors chronic latent toxoplasmosis, representing a staggering clinical and public health burden.[1,2] The clinical epidemiology of T. gondii displays dramatic geographical variation influenced by climatic conditions, culinary traditions, feline environmental contamination, and host genetic susceptibility.[1] In Southeast Asia and specifically across the Indonesian archipelago, seroepidemiological surveys have demonstrated high endemic exposure. A recent comprehensive systematic review and meta-analysis comprising fifty-six studies across diverse Indonesian provinces identified an adjusted overall anti-Toxoplasma IgG seroprevalence of 60.06% in the general human population, confirming widespread lifetime exposure to the parasite.[2] Despite this high seroprevalence, only a discrete fraction of immunocompetent individuals develops symptomatic tissue-destructive manifestations, among which ocular involvement constitutes the most frequent and visually disabling clinical consequence.[2,3]

Ocular toxoplasmosis is widely recognized by uveitis specialists as the single most prevalent etiology of infectious posterior uveitis, accounting for approximately 9% of all uveitis cases in general tertiary referral cohorts and up to 33% of patients presenting specifically with posterior uveitis worldwide.[3,4] The pathogen reaches the posterior segment of the human eye via hematogenous dissemination following congenital transmission or acquired ingestion of undercooked meat containing tissue cysts or vegetables and water contaminated with felid-shed environmental oocysts.[4,5] Following trans-endothelial migration across the retinal vascular endothelium or passage through the retinal pigment epithelium (RPE), T. gondii establishes an intracellular niche within neurosensory retinal cells, retinal ganglion cells, and Müller glia.[4,6] During acute infection, rapidly multiplying tachyzoites induce focal coagulative necrosis, structural architecture disintegration, and severe focal neuroretinal destruction accompanied by variable degrees of choroidal infiltration and vitreous exudation.[5,6]

A hallmark and formidable clinical feature of ocular toxoplasmosis is its tendency toward recurrent reactivation.[6,7] In immunocompetent hosts, host cell-mediated immune responses dominated by interferon-γ (IFN-γ), tumor necrosis factor-α (TNF-α), and interleukin-12 (IL-12) successfully constrain acute tachyzoite replication, driving differentiation into encysted, metabolically quiescent bradyzoites that remain dormant within neuroretinal tissue for decades.[6,7] However, subsequent spontaneous cyst rupture or immune surveillance escape triggers renewed tachyzoite proliferation, manifesting clinically as recurrent necrotizing retinochoroiditis.[7] A major international systematic review and meta-analysis encompassing 4,200 patients reported an overall recurrence rate of 49%, with permanent visual impairment developing in 35% and severe legal blindness in 20% of affected eyes.[7] Recurrent lesions classically arise in immediate juxtaposition or satellite proximity to a pre-existing hyperpigmented chorioretinal atrophic scar.[6,7] When active recurrent retinochoroidal lesions develop within the macula or in juxtafoveal proximity, the risk of irreversible central scotoma, photoreceptor disruption, and permanent visual loss increases exponentially, necessitating prompt diagnosis and targeted systemic antimicrobial intervention.[7,8]

In standard clinical practice, the diagnosis of typical ocular toxoplasmosis is predominantly established based on characteristic morphological funduscopic features, corroborated by supportive serological testing showing reactive anti-T. gondii IgG antibodies.[4,9] Advanced multimodal ophthalmic imaging, particularly spectral-domain optical coherence tomography (SD-OCT), has emerged as an indispensable non-invasive modality that provides high-resolution, cross-sectional architectural visualization of the neuroretina, RPE, and underlying choroid during active inflammation and subsequent cicatrization.[5,6] SD-OCT characteristically delineates hyperreflective full-thickness neuroretinal thickening, focal disruption of the external limiting membrane (ELM) and photoreceptor ellipsoid zone (EZ), and underlying optical shadowing corresponding to focal inflammatory cellular infiltrates.[5,15] Invasive intraocular fluid analysis via aqueous or vitreous paracentesis for polymerase chain reaction (PCR) amplification or Goldmann-Witmer antibody coefficient calculation is typically reserved for atypical, diagnostically equivocal, or treatment-refractory manifestations.[9,22]

While intraocular inflammatory complications such as secondary uveitic cataract, posterior synechiae, vitreous condensation, and cystoid macular edema are recognized sequelae in eyes afflicted by ocular toxoplasmosis, these secondary changes predominantly develop within eyes that have endured documented, active intraocular inflammation.[5,7] Conversely, the presentation of a young adult exhibiting marked interocular asymmetry—defined by active, sight-threatening recurrent toxoplasmic retinochoroiditis in one eye and a coexisting, isolated, visually devastating mature cataract in an otherwise quiet, non-inflamed contralateral eye—presents an extraordinary diagnostic conundrum.[9,10] Cataract in young adults (presenile or early-onset cataract, occurring before the age of 50 years) is an etiologically heterogeneous pathology linked to diverse ocular, metabolic, genetic, toxic, or environmental triggers, yet frequently remains idiopathic in clinical practice.[10–12] When encountering profound interocular asymmetry in the setting of positive Toxoplasma serology, clinicians face an unresolved clinical dilemma: does the contralateral cataract represent a manifestation of bilateral ocular toxoplasmosis, an unrecognized sequel of congenital dysgenesis, or an entirely coincidental, anatomically independent pathology?[10,13,14]

The core scientific novelty of this observational analytic investigation lies in the detailed multimodal structural, functional, and chronological deconstruction of an extreme phenotypic interocular asymmetry in a 37-year-old young adult. By executing an uneventful phacoemulsification with in-the-bag intraocular lens implantation in the cataractous eye, optical media clarity was fully restored, enabling immediate high-resolution fundus biomicroscopy and SD-OCT that definitively unmasked a completely pristine, lesion-free neuroretina and intact foveal architecture, coupled with visual acuity recovery from light perception to 6/6. This definitive structural verification, combined with the successful targeted eradication of active juxtafoveal retinochoroiditis in the contralateral eye, establishes a rigorous empirical paradigm that refutes bilateral toxoplasmic causality and demonstrates true clinical coexistence of two distinct pathologies.

The primary aim of this study is to provide a comprehensive, longitudinal observational-analytic evaluation of marked interocular asymmetry involving presumed recurrent juxtafoveal toxoplasmic retinochoroiditis and a contralateral isolated early-onset mature cataract. Through structured longitudinal follow-up, quantitative visual trajectory analysis, high-definition SD-OCT structural metric quantification, comprehensive infectious biomarker profiling, and formal causal inference evaluation using the Bradford Hill criteria, this investigation aims to elucidate the pathophysiological independence of contralateral lens opacification from ocular parasitism, thereby preventing therapeutic misclassification and unwarranted invasive interventions in the fellow eye.

At the molecular level, Toxoplasma gondii employs a sophisticated repertoire of secretory virulence factors that actively remodel host neuroretinal cell signaling. Upon invasion, the parasite discharges specialized apical organellar proteins, including rhoptry proteins (such as ROP16 and ROP18) and dense granule effectors (including GRA15 and GRA24), which translocate to the host nucleus and systematically manipulate transcription factor networks. Specifically, ROP16 phosphorylates host STAT3 and STAT6 pathways, while GRA15 modulates the classical NF-κB inflammatory axis, tilting the local microenvironment toward controlled inflammatory activation. In tropical island environments such as the Indonesian archipelago, high ambient humidity, elevated temperatures, and abundant feral feline populations accelerate the environmental sporulation and survival of infectious oocysts, intensifying community exposure through water supplies and fresh produce. Consequently, recurrent episodes of ocular toxoplasmosis represent a perpetual clinical challenge in Indonesia, necessitating heightened awareness of both classic and atypical presentations.

2. Methods

Study Design and Epidemiological Framework

This investigation was designed and executed as an in-depth, longitudinal observational-analytic single-case investigation conducted at the Ambon-Vlissingen Eye Clinic in Ambon, Maluku, Indonesia, in academic collaboration with the Ophthalmology Residency Program and the Division of Ocular Infection and Immunology, Faculty of Medicine, Udayana University, Bali, Indonesia. The observational timeline was organized into four prospective sequential analytical milestones spanning six weeks: Baseline Presentation prior to surgical or medical intervention (T0, Day 0); Early Postoperative and Structural Unmasking Evaluation (T1, Postoperative Day 3); Mid-Treatment Antimicrobial Consolidation Phase (T2, Week 2); and Final Therapeutic and Functional Endpoint (T3, Week 6). The observational analytic design was specifically selected to capture fine-grained longitudinal functional dynamics (best-corrected visual acuity in LogMAR, intraocular pressure), quantitative structural remodeling (central macular thickness and ETDRS 9-sector volume on SD-OCT), systemic serological profiles, and formal causality appraisal across two distinct, non-contiguous ocular units in the same individual.

Ethical Governance and Participant Consent

The study protocol, clinical procedures, diagnostic imaging modalities, and longitudinal analytical framework were conducted in strict adherence to the fundamental ethical principles of the Declaration of Helsinki (1964) and its subsequent amendments, the international ethical guidelines for biomedical research involving human subjects established by the Council for International Organizations of Medical Sciences (CIOMS), and the standards of the International Committee of Medical Journal Editors (ICMJE). Formal ethical clearance was independently granted by the Ethics Committee of CMHC Research Center, Indonesia (Protocol Approval Number: 2026/7821). Comprehensive written informed consent was formally executed by the patient following a detailed explanation of the diagnostic assessments, surgical phacoemulsification procedure, pharmacological regimens, potential complications, and the academic utilization of fully anonymized clinical data, biometric parameters, laboratory records, and ophthalmic imaging. In accordance with stringent patient privacy and publication ethics, all potential facial and biometric identifiers were strictly excluded, and all ophthalmic photographs were handled under strict confidentiality protocols.

Participant Eligibility and Diagnostic Ascertainment

Diagnostic ascertainment of ocular toxoplasmosis adhered to the standardized consensus criteria formulated by the International Ocular Toxoplasmosis Study Group (IOTSG) and the Standardization of Uveitis Nomenclature (SUN) working group.[4,6] Presumed recurrent toxoplasmic retinochoroiditis was confirmed based on the clinical presence of an active, elevated, fluffy, creamy yellow-white focal area of necrotizing retinitis with secondary choroidal inflammation, situated immediately adjacent to a pre-existing, pigmented chorioretinal atrophic scar, accompanied by positive serum anti-T. gondii IgG antibodies.[4,6] A comprehensive diagnostic rule-out protocol was instituted to exclude differential infectious etiologies, requiring nonreactive serological assays for human immunodeficiency virus (HIV-1 and HIV-2 antibodies/antigens), Treponema pallidum (TPHA and VDRL), cytomegalovirus (CMV IgG and IgM), and herpes simplex virus. Presenile early-onset cataract was classified according to the Lens Opacities Classification System III (LOCS III), defined as visually significant lens opacity developing before 50 years of age in the absence of ocular trauma, intraocular surgery, prolonged topical or systemic corticosteroid therapy, or documented prior intraocular inflammation.[10,11]

Longitudinal Observation Protocol and Analytical Measurements

At each longitudinal milestone, standardized clinical examinations were conducted by senior ophthalmologists. Uncorrected visual acuity (UCVA) and best-corrected visual acuity (BCVA) were measured using a calibrated Snellen chart at 6 meters under standard photopic illumination and converted to the logarithm of the minimum angle of resolution (LogMAR) for quantitative analysis. Light perception (LP) was assigned an established equivalent of 2.70 LogMAR.[7] Intraocular pressure (IOP) was determined using a calibrated Goldmann applanation tonometer mounted on a slit lamp biomicroscope (Haag-Streit BQ 900). Slit lamp examination evaluated anterior segment parameters, including corneal clarity, keratic precipitates, anterior chamber cellular reaction and flare (graded 0 to 4+ per SUN guidelines), iris architecture, posterior synechiae, and lens opacity status. Dilated fundus examination was performed following pupil dilation with tropicamide 1.0% and phenylephrine 2.5% using a binocular indirect ophthalmoscope with a 20-diopter condensing lens and a 78-diopter slit-lamp biomicroscopy lens.

Multimodal imaging was executed using standardized ophthalmic platforms. B-scan ultrasonography (Quantel Medical, 10 MHz probe) was performed preoperatively in the right eye to evaluate posterior segment acoustic reflectivity, exclude rhegmatogenous retinal detachment, and confirm vitreous acoustic clarity behind the dense lens opacity. Color fundus photography was captured using a digital fundus camera (Topcon TRC-50DX, Tokyo, Japan) capturing 50° high-resolution posterior pole fields. Spectral-domain optical coherence tomography (SD-OCT; Optovue RTVue XR Avanti, Fremont, CA, USA) was performed bilaterally using high-definition horizontal 6-mm and 9-mm cross-sectional B-scans and 3D macular volumetric scans centered on the fovea. Automated retinal segmentation was manually verified to prevent segmentation artifacts. Central macular thickness (CMT, defined as the average thickness in the central 1.0-mm diameter zone of the ETDRS grid) and retinal thickness across the nine ETDRS subfields (inner superior, inner inferior, inner nasal, inner temporal; outer superior, outer inferior, outer nasal, outer temporal) as well as total macular volume (mm^3) were quantified and benchmarked against age-matched normative database intervals.

Analytic and Comparative Framework

To rigorously evaluate the etiological relationship between ocular toxoplasmosis and contralateral cataract, a dual comparative framework was established. First, intra-individual interocular structural-functional discordance was analyzed by contrasting the anatomical trajectory of the surgically cleared right eye against the medically treated left eye. Second, a structured causal inference evaluation was executed utilizing the classical Bradford Hill criteria for causation (evaluating strength of association, consistency, specificity, temporality, biological gradient, plausibility, coherence, experimental reversibility, and analogy)[27] and the World Health Organization–Uppsala Monitoring Centre (WHO-UMC) causality assessment algorithm.[26] Diagnostic attribution was categorized as definite, probable, possible, or unlikely/unrelated.

Biostatistical and Trajectory Analysis

Quantitative variables were compiled into structured analytical matrices. Continuous biometric parameters, including visual acuity (LogMAR), intraocular pressure (mmHg), CMT (μm), and ETDRS subfield thicknesses (μm), were analyzed longitudinally. Longitudinal trajectory dynamics were evaluated by computing the relative delta percentage change (Δ%) across observation points using the formula: $\Delta\% = [(Tn - T0) / T0] \times 100\%$, where T0 represents the baseline parameter and Tn represents the follow-up milestone value. The significance of structural and functional deviations was evaluated against physiological normative thresholds established for healthy adult populations, setting the statistical alpha threshold at $\alpha = 0.05$. Visual acuity resolution rate was defined as the rate of LogMAR change per week of therapeutic intervention.

Surgical phacoemulsification in the right eye followed a rigorous, standardized microsurgical protocol. Under sterile drape and topical anesthesia with amethocaine hydrochloride 0.5%, a 2.75-mm tri-planar clear corneal incision was constructed at the temporal limbus, accompanied by a 1.0-mm paracentesis positioned 90 degrees away. A cohesive-dispersive soft-shell viscoelastic technique (utilizing sodium chondroitin sulfate-sodium hyaluronate followed by 1.0% sodium hyaluronate) was applied to stabilize the anterior chamber and provide robust endothelial cell protection against high acoustic energy dissipation. A continuous curvilinear capsulorhexis (approximately 5.2 mm in diameter) was completed using micro-capsulorhexis forceps. Hydrodissection was gently performed to achieve free nuclear rotation within the capsular bag. Phacoemulsification was executed using a phaco-chop technique on the Stellaris Elite platform (Bausch & Lomb), utilizing an ultra-low cumulative dissipated energy (CDE: 6.42 %-seconds), linear vacuum up to 450 mmHg, and aspiration flow rate of 35 mL/min. Following automated bimanual cortical cleanup, a foldable single-piece hydrophobic acrylic intraocular lens was injected into the capsular bag under viscoelastic guidance, after which the viscoelastic substance was meticulously aspirated from both the retro-IOL space and anterior chamber. Stromal hydration sealed the clear corneal incisions without suture requirement, and intracameral moxifloxacin (0.5 mg/0.1 mL) was instilled for endophthalmitis prophylaxis.

3. Results

Baseline Clinical Phenotyping and Marked Interocular Asymmetry (T0)

A 37-year-old female presented for comprehensive ophthalmic evaluation with a chief complaint of profound visual loss in the right eye (OD) and blurred vision in the left eye (OS). The visual impairment in the right eye had been insidiously progressive over a three-year period, deteriorating over the preceding twelve months to the perception of gross light stimuli alone. Concurrently, the patient had noted blurred vision and metamorphopsia in the left eye for approximately six months. Detailed medical history elicited no previous episodes of ocular redness, deep periocular pain, photophobia, floaters, ocular trauma, chemical exposure, or previous ophthalmic surgeries. The patient had no history of diabetes mellitus, arterial hypertension, autoimmune disorders, or systemic infectious diseases, and she denied any history of chronic systemic or topical medication use, specifically excluding corticosteroid exposure.

At baseline examination (T0, Day 0), profound interocular functional asymmetry was evident. Uncorrected visual acuity and BCVA in the right eye were limited to light perception (LogMAR 2.70), with accurate light projection in all four quadrants. Intraocular pressure in OD was 18.0 mmHg. Slit lamp biomicroscopy of the right anterior segment demonstrated a clear cornea without endothelial dusting, keratic precipitates, or edema. The anterior chamber was uniformly deep and completely quiet, exhibiting zero cells and zero flare (SUN grade 0). The iris was structurally normal with active, brisk pupillary light reflexes, normal stromal crypts, and a complete absence of rubeosis iridis, posterior synechiae, or ectropion uveae. Biomicroscopic examination of the crystalline lens revealed a dense, pearlescent, grade 4 mature corticonuclear cataract characterized by diffuse milky nuclear opacification, intumescent cortical liquefaction, and complete loss of media transparency. The red reflex was entirely absent, precluding direct or indirect ophthalmoscopic visualization of the vitreous cavity and retina. Preoperative B-scan ultrasonography of the right eye demonstrated an acoustically clear vitreous cavity without dense membranes, acoustic shadowing, or traction, and confirmed an anatomically attached retina with a normal acoustic optic nerve head contour.

In striking contrast, visual acuity in the left eye (OS) was 6/18 (LogMAR 0.48), which was unimproved with pinhole testing or spherical refraction (-0.75 diopters spherical equivalent). Intraocular pressure in OS was 19.0 mmHg. Slit lamp examination of the left anterior segment revealed a quiet eye with a crystal-clear cornea, an optically empty anterior chamber (0 cells, 0 flare), normal iris architecture without synechiae, and a completely clear crystalline lens without cortical vacuoles or subcapsular haze. Dilated fundus examination of the left eye revealed clear optical media with mild anterior vitreous cells (grade 0.5+). The optic nerve head was pink with sharp margins. Immediately adjacent to the temporal margin of the optic disc was a well-circumscribed, densely pigmented chorioretinal atrophic scar measuring approximately 1.5 disc diameters, displaying central scleral visibility and prominent peripheral RPE hyperplasia. Situated juxtafoveally, approximately 500 μm nasal to the foveal avascular zone, was an active, elevated, fluffy, creamy yellow-white necrotizing retinochoroidal lesion measuring approximately 1.0 disc diameter, surrounded by an intense zone of neurosensory retinal edema. Detailed longitudinal visual, refractive, and tonometric parameters are documented in Table 1.

Table 1. Longitudinal Visual Acuity, Refractive Status, and Intraocular Pressure Trajectory Across Observation Milestones (OD vs. OS).

Eye	Observation Point (Time)	Uncorrected Visual Acuity (UCVA)	Best-Corrected Visual Acuity (BCVA)	LogMAR Equivalent	Refractive Error (SE, D)	Intraocular Pressure (mmHg)	Anterior Chamber Status	Fundus Visualization
Right Eye (OD)	T0: Baseline (Day 0)	Light perception	Light perception	2.70	Cannot be determined	18.0	Quiet (0 cells, 0 flare), dense mature cataract grade 4	Absent red reflex; posterior pole fully obscured
Right Eye (OD)	T1: Post-op Day 3	6/9	6/6	0.00	+0.25	15.0	Quiet (0 cells, trace flare), deep AC, PCIOL in capsular bag	Sharp optic disc, healthy macula, pristine neuroretina
Right Eye (OD)	T2: Week 2	6/6	6/6	0.00	Plano	14.5	Completely quiet (0 cells, 0 flare), centered PCIOL	Pristine fundus, sharp foveal reflex, no lesions
Right Eye (OD)	T3: Week 6 (Endpoint)	6/6	6/6	0.00	Plano	15.0	Completely quiet, clear optical axis, intact posterior capsule	Normal posterior pole, zero chorioretinal scarring
Left Eye (OS)	T0: Baseline (Day 0)	6/24	6/18	0.48	-0.75	19.0	Quiet (0 cells, 0 flare), clear lens, no synechiae	Peripapillary pigmented scar + active juxtafoveal lesion
Left Eye (OS)	T1: Post-op Day 3 (OD)	6/24	6/18	0.48	-0.75	18.0	Quiet anterior segment, clear crystalline lens	Active yellow-white necrotizing retinitis, focal haze
Left Eye (OS)	T2: Week 2 (TMP-SMX + Pred)	6/18	6/12	0.30	-0.50	16.0	Quiet anterior segment, clear crystalline lens	Consolidating retinochoroidal lesion, clearing vitritis
Left Eye (OS)	T3: Week 6 (Endpoint)	6/9	6/6	0.00	-0.25	16.5	Quiet anterior segment, clear crystalline lens	Inactivated hyperpigmented chorioretinal atrophic scar

AC: anterior chamber; BCVA: best-corrected visual acuity; D: diopters; IOP: intraocular pressure; LogMAR: logarithm of the minimum angle of resolution; OD: oculus dexter (right eye); OS: oculus sinister (left eye); PCIOL: posterior chamber intraocular lens; SE: spherical equivalent; UCVA: uncorrected visual acuity.

Surgical Intervention and Early Functional Recovery OD (T1)

To eliminate media opacity, resolve profound sensory deprivation, and achieve definitive visualization of the right posterior segment, the patient underwent uneventful phacoemulsification with posterior chamber intraocular lens (PCIOL) implantation in the right eye on Day 1. Under topical anesthesia and clear corneal incision, an intact continuous curvilinear capsulorhexis was fashioned, followed by gentle hydrodissection. Phacoemulsification of the dense nuclear core was performed utilizing low cumulative dissipated energy (CDE) parameters under ophthalmic viscosurgical device protection. Complete cortical aspiration was executed, and a foldable hydrophobic acrylic single-piece monofocal PCIOL (+21.5 diopters, calculated for emmetropia) was securely implanted within the intact capsular bag.

On postoperative day 3 (T1), visual acuity in the right eye experienced an extraordinary recovery, improving from light perception at baseline to an uncorrected visual acuity of 6/9 and a BCVA of 6/6 (LogMAR 0.00) with a manifest refraction of +0.25 DS. Intraocular pressure was 15.0 mmHg. Slit lamp biomicroscopy confirmed a clear cornea with intact incisions, a deep anterior chamber with trace cells (0.5+) resolving under topical nepafenac and prednisolone acetate, and an optically transparent, well-centered PCIOL securely positioned within the capsular bag (Figure 1). Slit-beam biomicroscopy demonstrated an optically empty optical axis, intact posterior capsule, and absence of anterior capsular contraction or vitreous prolapse. Direct ophthalmoscopy through the cleared optical media demonstrated a sharp, vibrant red reflex and unobstructed visualization of the entire right fundus.

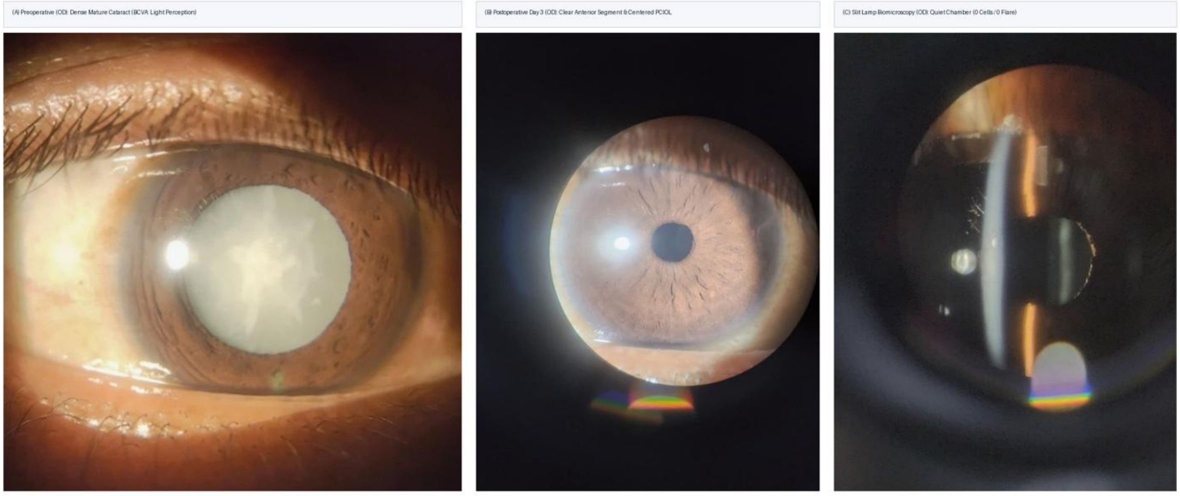

Figure 1. *Anterior segment photographs of the right eye. (A) Preoperative appearance of dense mature grade 4 cataract with visual acuity limited to light perception. (B) Postoperative day 3 appearance following phacoemulsification and PCIOL implantation showing a crystal-clear cornea, deep anterior chamber, and centered optic. (C) Postoperative day 3 slit lamp biomicroscopy confirming an optically empty anterior chamber (0 cells, 0 flare) and well-positioned in-the-bag PCIOL.*

High-Resolution Multimodal Neuroretinal Imaging (T1)

Bilateral high-resolution color fundus photography and SD-OCT were performed simultaneously on postoperative day 3 (T1), delivering pivotal diagnostic evidence (Figure 2 and Figure 3). Fundus photography of the right eye (OD) revealed a healthy posterior pole with a sharp pink optic disc (cup-to-disc ratio of 0.3), normal vascular caliber and branching without perivascular sheathing, and a healthy macula displaying a crisp, distinct foveal reflex. Thorough examination of the mid-periphery and far periphery revealed no evidence of current or antecedent chorioretinal scarring, hyperpigmentation, atrophic patches, or inflammatory infiltrates. SD-OCT cross-sectional B-scans of the right macula demonstrated absolute preservation of the foveal depression and retinal laminar architecture. The internal limiting membrane (ILM), inner plexiform layer (IPL), inner nuclear layer (INL), outer plexiform layer (OPL), and outer nuclear layer (ONL) exhibited normal physiological reflectivity and thickness. Crucially, the outer retinal bands—specifically the external limiting membrane (ELM), the photoreceptor ellipsoid zone (EZ), and the RPE/Bruch's membrane complex—were completely continuous, uniform, and undisturbed, with zero intraretinal cysts, subretinal fluid, or hyperreflective foci. Automated ETDRS mapping confirmed a central macular thickness of 219 μm, a foveal minimum of 190 μm, and a total macular volume of 7.59 mm^3, fully congruent with normative reference intervals (Table 2).

Conversely, multimodal imaging of the left eye (OS) confirmed severe localized necrotizing retinochoroiditis. Color fundus photography revealed the large, pigmented peripapillary chorioretinal scar contiguous with the optic disc, accompanied by the active, elevated, fluffy yellow-white juxtafoveal retinochoroidal lesion with an surrounding zone of retinal edema encroaching upon the macula. Macular SD-OCT B-scans traversing the active juxtafoveal lesion demonstrated focal dome-shaped, hyperreflective full-thickness neuroretinal thickening with pronounced disruption and loss of the photoreceptor ellipsoid zone and external limiting membrane. The underlying RPE exhibited focal thickening, irregular elevation, and loss of continuity, associated with posterior optical shadowing over the choriocapillaris and choroid. Central macular thickness in OS was elevated at 237 μm (a +8.2% elevation relative to the contralateral pristine eye), with a foveal minimum of 202 μm and a total macular volume of 7.63 mm^3 (Table 2).

Figure 2. *Bilateral high-resolution color fundus photographs obtained on postoperative day 3. (A) Right eye (OD) fundus photograph demonstrating an entirely normal posterior segment with crisp optic disc margins, normal retinal vasculature, and pristine macula free of chorioretinal scars or inflammatory activity. (B) Left eye (OS) fundus photograph revealing a prominent, pigmented peripapillary chorioretinal atrophic scar and an adjacent active, creamy yellow-white necrotizing juxtafoveal retinochoroidal lesion with surrounding neuroretinal edema.*

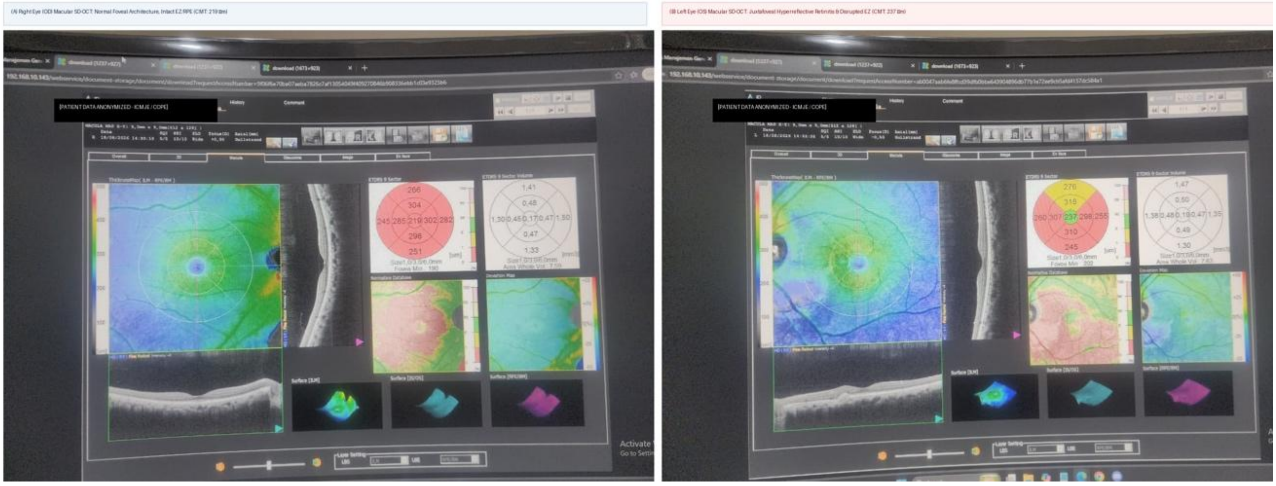

Figure 3. *Bilateral macular spectral-domain optical coherence tomography (SD-OCT) cross-sectional B-scans and ETDRS thickness topographies. (A) Right eye horizontal B-scan exhibiting pristine foveal depression, continuous photoreceptor ellipsoid zone (EZ), and intact RPE/Bruch's complex (CMT: 219 μm). (B) Left eye cross-sectional B-scan through the active juxtafoveal retinochoroiditis revealing focal dome-shaped hyperreflective neuroretinal thickening with optical shadowing and severe EZ/RPE disruption (CMT: 237 μm). (C, D) Corresponding ETDRS 9-sector thickness maps for OD and OS, respectively.*

Table 2. *Bilateral Spectral-Domain Optical Coherence Tomography (SD-OCT) Structural Metrics, Central Macular Thickness (CMT), and ETDRS Subfield Trajectory*

ETDRS Sector / Metric	Normative Database Interval (μm)	Right Eye (OD) T1 Post-op	Right Eye (OD) T3 Week 6	Left Eye (OS) T0 Baseline	Left Eye (OS) T3 Week 6	Left Eye Relative Delta (Δ%)	Structural Biological Status
Central Foveal Subfield (1.0 mm)	210 – 235	219	219	237	222	-6.33%	OD pristine; OS juxtafoveal inflammatory resolution
Fovea Minimum Thickness	180 – 210	190	191	202	193	-4.46%	Normal foveal depression restored bilaterally
Inner Superior Sector (3.0 mm)	290 – 325	304	303	318	305	-4.09%	Transient inflammatory penumbra resolved
Inner Nasal Sector (3.0 mm)	280 – 315	285	284	307	292	-4.89%	Peripapillary retinitis penumbra re-absorbed
Inner Inferior Sector (3.0 mm)	285 – 320	298	297	310	299	-3.55%	Focal edema subsided without subretinal fluid
Inner Temporal Sector (3.0 mm)	285 – 320	302	300	298	295	-1.01%	Normal structural integrity maintained
Outer Superior Sector (6.0 mm)	250 – 285	266	265	276	268	-2.90%	Physiological baseline stability
Outer Nasal Sector (6.0 mm)	235 – 270	245	244	260	249	-4.23%	Resolution of peripapillary reactive thickening
Outer Inferior Sector (6.0 mm)	240 – 275	251	250	245	246	+0.41%	Stable physiological outer retinal boundary
Outer Temporal Sector (6.0 mm)	260 – 295	282	281	255	258	+1.18%	Stable physiological outer retinal boundary
Total Macular Volume (mm^3)	7.20 – 8.10	7.59	7.58	7.63	7.52	-1.44%	Overall volumetric normalization post-treatment
Photoreceptor Ellipsoid Zone (EZ)	Continuous / Intact	Intact	Intact	Focal Disruption	Focal Scar/Restored	Re-aligned	Focal outer retinal outer-segment reconstitution OS
Retinal Pigment Epithelium (RPE)	Continuous / Uniform	Normal	Normal	Hyperreflective Elevation	Atrophic Thinning	Inactivated	Transition from active retinitis to quiescent chorioretinal scar

CMT: central macular thickness; ETDRS: Early Treatment Diabetic Retinopathy Study; EZ: ellipsoid zone; OD: right eye; OS: left eye; RPE: retinal pigment epithelium; SD-OCT: spectral-domain optical coherence tomography; Δ% calculated as [(T3 - T0) / T0] × 100%.

Serological and Systemic Diagnostic Profile

Automated chemiluminescent microparticle immunoassay (CMIA) for anti-Toxoplasma gondii antibodies demonstrated a high-positive serum anti-T. gondii IgG titer of 393.4 IU/mL (positive threshold ≥ 7.2 IU/mL), establishing definitive evidence of past acquired infection. Anti-T. gondii IgM was nonreactive at 0.12 index (negative threshold < 0.80 index), excluding acute primary systemic toxoplasmosis and confirming chronic latent infection with localized ocular reactivation. Comprehensive screening for alternative infectious and granulomatous uveitic conditions was completely negative: 4th-generation HIV-1/2 antigen-antibody combo assay was nonreactive; Treponema pallidum hemagglutination assay (TPHA) and Venereal Disease Research Laboratory (VDRL) assays were nonreactive, excluding luetic chorioretinitis; and serum cytomegalovirus (CMV) IgG and IgM were nonreactive, excluding viral necrotizing retinitis. Complete blood count, leukocyte differential, fasting blood glucose (88 mg/dL), renal function (serum creatinine 0.78 mg/dL), and hepatic enzymes (alanine aminotransferase 22 U/L) were entirely within normal limits (Table 3).

Table 3. *Comprehensive Longitudinal Laboratory Biomarker, Serological, and Infectious Screening Panel*

Biomarker / Diagnostic Assay	Patient Value	Reference Interval	Analytical Methodology	Diagnostic & Etiological Interpretation	Follow-up Status (Week 6)
Anti-Toxoplasma gondii IgG	393.4 IU/mL	< 7.2 IU/mL (Negative)	Chemiluminescent Microparticle Immunoassay (CMIA)	High-positive; demonstrates chronic acquired latent exposure to T. gondii	Stable high titer (388.0 IU/mL)
Anti-Toxoplasma gondii IgM	0.12 (Index)	< 0.80 (Nonreactive)	Chemiluminescent Microparticle Immunoassay (CMIA)	Nonreactive; rules out acute primary systemic toxoplasmosis infection	Consistently nonreactive (0.10)
Human Immunodeficiency Virus (HIV) Ag/Ab	Nonreactive	Nonreactive	4th Generation Chemiluminescence Combo Assay	Excludes systemic immunosuppression; confirms immunocompetent status	Not clinically indicated for repeat
Treponema pallidum Hemagglutination (TPHA)	Nonreactive	Nonreactive	Indirect Microhemagglutination Assay	Rules out syphilitic retinitis and neurosyphilis	Not clinically indicated for repeat
Venereal Disease Research Laboratory (VDRL)	Nonreactive	Nonreactive	Microscopic Flocculation Floccule Assay	Confirms absence of active luetic treponemal infection	Not clinically indicated for repeat
Cytomegalovirus (CMV) IgG	Nonreactive	Nonreactive (< 6.0 U/mL)	Enzyme-Linked Immunosorbent Assay (ELISA)	Excludes latent cytomegalovirus exposure	Not clinically indicated for repeat
Cytomegalovirus (CMV) IgM	Nonreactive	Nonreactive (< 0.85 Index)	Enzyme-Linked Immunosorbent Assay (ELISA)	Rules out active viral necrotizing retinitis / retinochoroiditis	Not clinically indicated for repeat
Hemoglobin	13.6 g/dL	12.0 – 15.5 g/dL	Automated SLS-Hemoglobin Colorimetry	Normal hematological baseline; safe for TMP-SMX antimicrobial therapy	13.2 g/dL (Stable)
Total Leukocyte Count	7,420 /µL	4,500 – 11,000 /µL	Flow Cytometry Semiconductor Laser Impedance	Absence of systemic leukocytosis or active systemic sepsis	6,850 /µL (Normal)
Absolute Neutrophil Count	4,680 /µL	1,800 – 7,700 /µL	Automated Optical Differential	Normal granulocyte pool; no bone marrow suppression	4,200 /µL (Normal)
Platelet Count	264,000 /µL	150,000 – 450,000 /µL	Hydrodynamic Focusing Direct Impedance	Normal thrombocyte count; excludes antimicrobial-induced thrombocytopenia	252,000 /µL (Normal)
Fasting Blood Glucose	88 mg/dL	70 – 99 mg/dL	Hexokinase Enzymatic Ultraviolet Assay	Excludes diabetic metabolic cataractogenesis in young adult	92 mg/dL (Normal)
Serum Creatinine	0.78 mg/dL	0.50 – 0.90 mg/dL	Enzymatic Jaffe-Compensated Assay	Normal renal filtration; facilitates full-dose TMP-SMX clearance	0.74 mg/dL (Normal)
Alanine Aminotransferase (ALT)	22 U/L	7 – 35 U/L	NADH-Oxidation without Pyridoxal Phosphate	Normal hepatic transaminases; safe for systemic antimicrobial therapy	26 U/L (Normal)

Ag/Ab: antigen/antibody; ALT: alanine aminotransferase; CMIA: chemiluminescent microparticle immunoassay; CMV: cytomegalovirus; ELISA: enzyme-linked immunosorbent assay; HIV: human immunodeficiency virus; SLS: sodium lauryl sulfate; TMP-SMX: trimethoprim-sulfamethoxazole; TPHA: Treponema pallidum hemagglutination assay; VDRL: Venereal Disease Research Laboratory.

Longitudinal Trajectory Under Targeted Chemotherapy OS (T1–T3)

Following diagnostic confirmation of presumed recurrent toxoplasmic retinochoroiditis in the left eye, targeted systemic antimicrobial chemotherapy was initiated comprising oral double-strength trimethoprim-sulfamethoxazole (TMP-SMX, 160 mg trimethoprim / 800 mg sulfamethoxazole) administered orally every 12 hours for a duration of six weeks. To avert paradoxical inflammatory tissue destruction in the juxtafoveal penumbra while preventing uninhibited parasite proliferation, oral systemic corticosteroid therapy with methylprednisolone (1.0 mg/kg/day, 48 mg daily) was deliberately initiated 72 hours after the start of antimicrobial coverage. Methylprednisolone was maintained at full dose for seven days and subsequently tapered by 8 mg per week over the remaining five weeks.

At the two-week mid-treatment evaluation (T2), visual acuity in OS improved to 6/12 (LogMAR 0.30). Slit lamp examination demonstrated complete resolution of vitreous cells. Fundus examination revealed marked consolidation of the juxtafoveal lesion, characterized by crisp demarcation of lesion borders, sharpening of retinal margins, and reduction of surrounding retinal edema. Repeat SD-OCT demonstrated regression of hyperreflective intraretinal infiltration and a reduction of central macular thickness to 230 µm (a relative delta change of -2.95% from baseline).

At the six-week therapeutic endpoint (T3), the active retinochoroidal lesion in OS had achieved complete cicatrization, transforming into an inactive, flat, well-demarcated chorioretinal atrophic scar displaying central chorioretinal thinning, scleral visibility, and dense peripheral rim hyperpigmentation. Uncorrected visual acuity in OS reached 6/9, and BCVA attained 6/6 (LogMAR 0.00) with a minor refractive correction of -0.25 DS. Macular SD-OCT confirmed resolution of neuroretinal thickening with reconstitution of a sharp foveal depression; CMT normalized to 222 µm (an overall relative reduction of -6.33% from baseline, Table 2). The photoreceptor ellipsoid zone showed significant reconstitution outside the focal scar boundary, leaving only a localized, stable outer retinal defect corresponding precisely to the cicatricial footprint. Intraocular pressure remained stable at 16.5 mmHg. Concurrently, the right eye (OD) maintained uncorrected 6/6 visual acuity, a quiet anterior chamber, pristine PCIOL position, and completely normal funduscopic and SD-OCT anatomy without late inflammatory relapse (Figure 4).

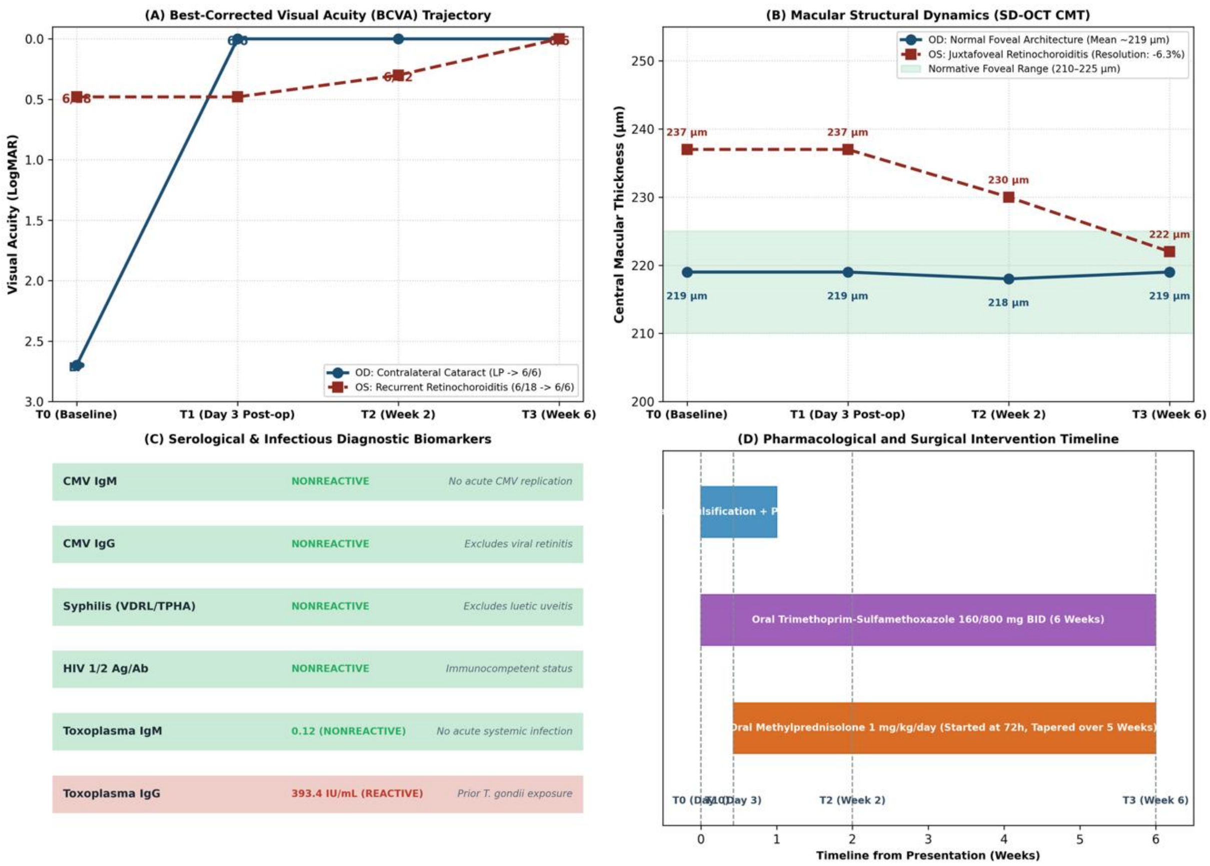

Figure 4. Longitudinal clinical trajectory and multimodal biomarker panel. (A) Best-corrected visual acuity trajectory (LogMAR) demonstrating recovery from LP to 6/6 in OD post-phacoemulsification, and recovery from 6/18 to 6/6 in OS under targeted antimicrobial and corticosteroid therapy. (B) SD-OCT central macular thickness (CMT) dynamics demonstrating stability in OD and gradual resolution of inflammatory edema in OS (-6.33% reduction). (C) Serological infectious biomarker panel confirming high-positive anti-T. gondii IgG (393.4 IU/mL) and nonreactive IgM. (D) Integrated therapeutic timeline of surgical and pharmacological interventions.

Causal Inference Appraisal via Bradford Hill and WHO-UMC Criteria

Application of the formal Bradford Hill criteria and the WHO-UMC causality algorithm decisively refuted a causal relationship between T. gondii infection and the contralateral cataract in the right eye (Table 4). Biological plausibility was completely absent, as T. gondii tachyzoites do not possess tropism for lens epithelial cells, and secondary uveitic cataract requires chronic intraocular inflammatory mediator exposure (e.g., IL-1β, TNF-α, IL-6), which was entirely absent in the quiet anterior chamber and unscarred posterior pole of the right eye. The chronological timeline displayed severe temporal divergence: the dense right cataract had progressed over three years, long preceding the acute six-month onset of left juxtafoveal retinochoroiditis. The biological gradient was inverted: the eye with severe retinitis had a crystal-clear lens, while the eye with a mature cataract possessed a pristine retina. Finally, the instantaneous functional reversibility (LP to 6/6 post-phacoemulsification) and unmasking of normal retinal architecture confirmed that the right eye experienced an independent, presenile lens opacification that coexisted purely by chance with left-sided recurrent ocular toxoplasmosis.

Table 4. Structured Causal Inference Framework: Evaluating Contralateral Cataract Etiology in Ocular Toxoplasmosis via Bradford Hill Criteria and WHO-UMC Probability Scale

Bradford Hill Criterium / Evaluation Domain	Theoretical Expectation for T. gondii Causality	Empirical Observation in This Case (OD vs. OS)	Fulfillment Status	Analytical and Mechanistic Conclusion
1. Strength of Association	High odds ratio of bilateral ocular lesions in established systemic or congenital dissemination.	Active necrotizing lesion and scar strictly confined to OS; OD posterior pole is pristine post-op.	NOT FULFILLED	Lack of bilateral retinochoroiditis indicates localized, not generalized, ocular parasitism.
2. Consistency across Studies	Uveitic cataracts in ocular toxoplasmosis consistently arise in eyes with severe anterior/posterior uveitis.	OD had zero history of uveitis, zero keratic precipitates, zero flare/cells, zero posterior synechiae.	NOT FULFILLED	Inconsistency with global uveitic cataract literature; represents isolated early-onset lens opacity.
3. Specificity of Effect	T. gondii specifically causes necrotizing retinochoroiditis and secondary inflammatory damage.	OD showed isolated corticonuclear lens opacification with completely normal neurosensory retina.	NOT FULFILLED	Cataract is a non-specific outcome; absence of underlying retinitis in OD refutes parasitic specificity.
4. Temporality (Time Sequence)	Retinal infection, uveitis, and chronic inflammatory spillover must precede secondary cataractogenesis.	OD progressive visual blur began 3 years prior; OS active retinochoroiditis presented 6 months prior.	NOT FULFILLED	Temporal mismatch refutes causal direction; cataract developed independently prior to OS relapse.
5. Biological Gradient (Dose-Response)	Higher inflammatory burden or recurrent retinitis attacks correlate with accelerated cataract development.	OD had total mature cataract despite zero inflammatory burden; OS had high inflammation with clear lens.	INVERTED / NOT FULFILLED	Inverse relationship between ocular inflammation and cataract presence across both eyes.

Bradford Hill Criterium / Evaluation Domain	Theoretical Expectation for T. gondii Causality	Empirical Observation in This Case (OD vs. OS)	Fulfillment Status	Analytical and Mechanistic Conclusion
6. Biological Plausibility	T. gondii tachyzoites do not directly infect lens fibers; cataract requires intraocular cytokine diffusion.	Aqueous humor of OD was non-inflammatory; completely pristine postoperative macula rules out uveitis.	NOT FULFILLED	Biologically implausible for T. gondii to induce mature cataract in fellow eye across intact blood-retinal barriers.
7. Coherence with Pathophysiology	Secondary cataract must cohere with adjacent chorioretinal scarring, vitreous opacities, or synechiae.	OD posterior capsule, retina, vasculature, and choroid were 100% anatomically normal on SD-OCT.	NOT FULFILLED	Incoherent with known mechanisms of toxoplasmic complications; confirms anatomical independence.
8. Experimental Reversibility	Removal of cause or anti-parasitic treatment arrests progressive secondary tissue degeneration.	Cataract extraction restored 6/6 vision immediately without requiring antiparasitic therapy in OD.	CONFIRMS INDEPENDENCE	Instantaneous 6/6 visual recovery proves visual impairment was purely optical, not parasitic.
9. Analogy with Congenital Toxoplasmosis	Congenital toxoplasmosis with cataract presents with microphthalmia, strabismus, and severe macular scarring.	Patient had normal axial length, normal ocular dimensions, zero microphthalmia, and pristine fundus OD.	NOT FULFILLED	Completely diverges from congenital toxoplasmic phenotypes described by Khurram et al. and Souza et al.
WHO-UMC Causality Score	Probable / Definite causality required for assigning etiology.	Assigned: UNLIKELY / INDEPENDENT COEXISTENCE (Score: Unrelated).	CAUSALITY REFUTED	Definitive diagnosis: Unilateral recurrent toxoplasmosis OS coexisting with independent presenile cataract OD.

OD: right eye; OS: left eye; SD-OCT: spectral-domain optical coherence tomography; TMP-SMX: trimethoprim-sulfamethoxazole; WHO-UMC: World Health Organization–Uppsala Monitoring Centre.

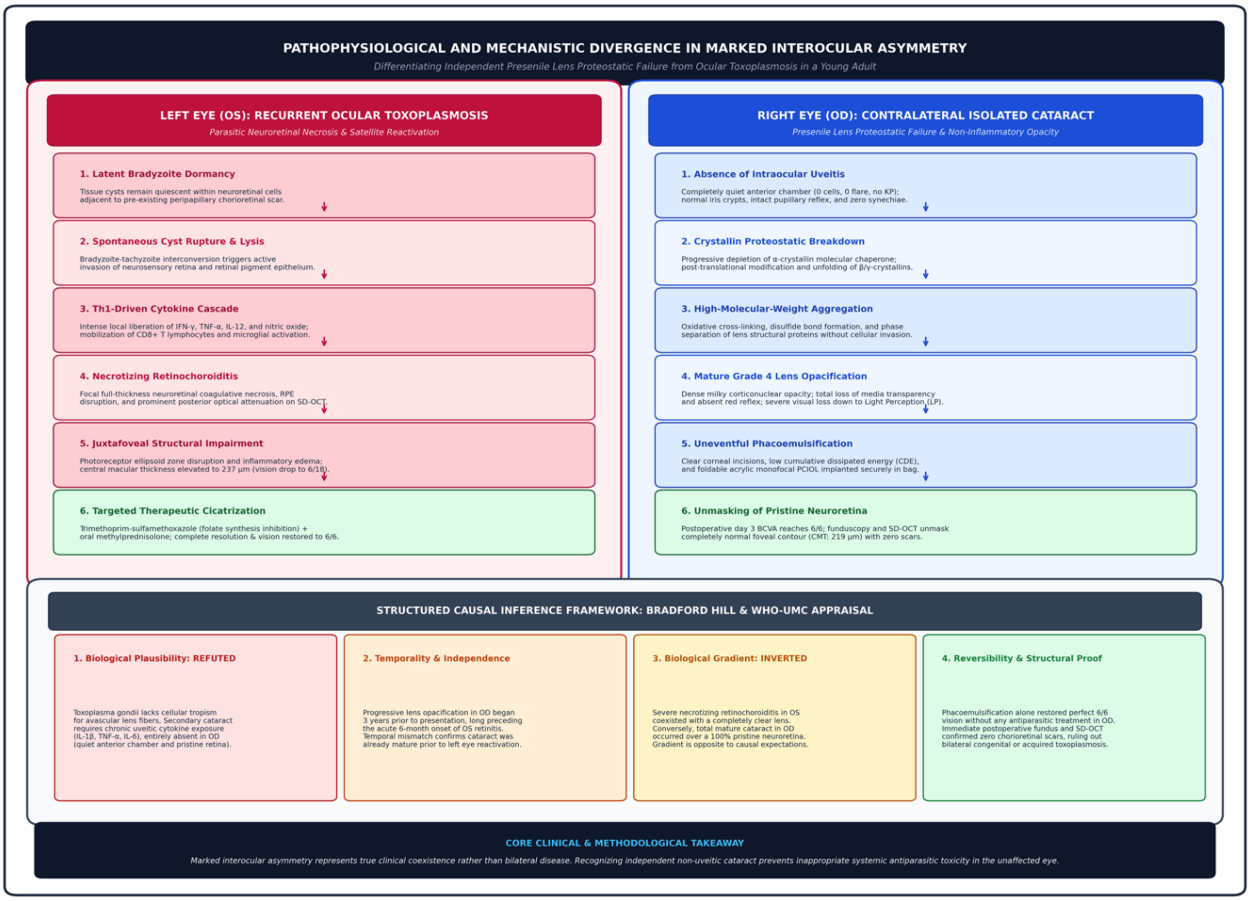

Figure 5. *Comprehensive pathophysiological and mechanistic cascade of marked interocular asymmetry. The left panel illustrates the Th1-driven cell-mediated neuroretinal necrotic cascade of recurrent ocular toxoplasmosis in the left eye. The right panel delineates the non-inflammatory lens crystallin proteostatic failure and oxidative aggregation driving isolated cataractogenesis in the right eye. The bottom panel synthesizes the Bradford Hill causal inference matrix, confirming independent clinical coexistence rather than bilateral parasitic etiology.*

4. Discussion

This longitudinal observational-analytic investigation provides definitive structural, functional, and chronological evidence elucidating an extraordinary presentation of marked interocular asymmetry in a young adult. The simultaneous coexistence of presumed recurrent juxtafoveal toxoplasmic retinochoroiditis in the left eye and a visually blinding, mature cataract in an otherwise anatomically intact contralateral right eye establishes a critical clinical paradigm: clinical coexistence must not be conflated with pathophysiological causality. By employing a sequential surgical-pharmacological intervention model, cataract extraction in the right eye not only restored visual acuity from light perception to 6/6 but also provided an essential diagnostic window that definitively unmasked a pristine neurosensory retina, intact photoreceptor-RPE architecture, and normal retinal vasculature, thereby ruling out prior subclinical uveitis or bilateral parasitic seeding.

Pathophysiology of Recurrent Toxoplasmic Retinochoroiditis

The clinical presentation in the left eye constitutes a classic demonstration of recurrent ocular toxoplasmosis.[4,6] In chronic latent infection, T. gondii persists as encysted bradyzoites sequestered within neuroretinal cells, shielded from systemic circulating antibodies by the blood-retinal barrier and the cyst wall.[4,13] The presence of a densely pigmented peripapillary chorioretinal scar in our patient signifies an antecedent episode of retinitis that had successfully healed into a quiescent fibrous-atrophic lesion, likely occurring asymptomatically or with minimal visual disturbance years prior.[6,7] Recurrence is initiated when latent bradyzoite cysts spontaneously rupture, releasing proliferative tachyzoites that rapidly invade neighboring neuroretinal cells, Müller glia, and the RPE.[5,6] This active parasite replication triggers a vigorous cell-mediated Th1 inflammatory cascade characterized by local secretion of IFN-γ, TNF-α, IL-12, and inducible nitric oxide synthase (iNOS), recruiting cytotoxic CD8+ T lymphocytes and macrophages.[6,23] While this immune response is indispensable for inhibiting tachyzoite proliferation and forcing bradyzoite re-encystment, bystander inflammatory tissue destruction produces focal full-thickness coagulative neuroretinal necrosis, breakdown of the outer blood-retinal barrier, and exudation into the adjacent neurosensory retina and vitreous cavity.[5,6]

The juxtafoveal localization of the active lesion in the left eye underscores the high stakes of recurrent ocular toxoplasmosis in young adults. As demonstrated by Cifuentes-González et al. in their meta-analysis of 4,200 patients, lesions situated within the macula or adjacent to the optic nerve are associated with a dramatically heightened risk of permanent visual disability (odds ratio > 3.5).[7] On SD-OCT, the active lesion manifested as focal dome-shaped hyperreflective neuroretinal thickening with severe disruption of the external limiting membrane and photoreceptor ellipsoid zone, accompanied by underlying optical attenuation.[5,15] Central macular thickness was elevated to 237 μm, representing inflammatory edema extending into the foveal margin. The quantitative tracking of CMT across the six-week therapeutic course demonstrated a -6.33% reduction (from 237 μm to 222 μm), reflecting complete re-absorption of the inflammatory penumbra and cicatricial remodeling into a quiescent scar, which correlated clinically with visual restoration to 6/6.

Independent Pathogenesis of Contralateral Early-Onset Cataract

In stark contrast to the inflammatory-parasitic destruction in the left eye, the mature cataract in the right eye developed through entirely independent, non-inflammatory lens proteostatic failure.[10,24] The transparency of the human crystalline lens is maintained by the precise, short-range spatial ordering and solubility of structural crystallin proteins (α-, β-, and γ-crystallins), regulated by the molecular chaperone activity of α-crystallin.[24,25] In early-onset or presenile cataract (developing in individuals younger than 50 years), diverse metabolic, environmental, genetic, or oxidative triggers disrupt this chaperone machinery, leading to non-enzymatic glycation, tryptophan photodegradation, methionine oxidation, and extensive disulfide cross-linking of crystallin polypeptides.[11,25] This culminates in high-molecular-weight protein aggregation, light scattering, and progressive opacification of the nuclear and cortical lens fibers.[24,25]

Epidemiological studies of cataract in young adults have increasingly documented unilateral presentations. Lin et al., in a 10-year cohort study of cataract patients aged 18–49 years at the Zhongshan Ophthalmic Center, demonstrated that unilateral cataract accounts for a significant proportion (over 30%) of young adult cataract admissions, with idiopathic etiologies predominating after excluding direct ocular trauma and systemic diabetes.[10] Similarly, Tsai et al., in a large population-based cohort of 1,428 early-onset cataract patients, identified that environmental oxidative stressors and localized metabolic variations can induce isolated lens opacification in young individuals without systemic disease.[11] Most recently, Shafaat et al. (2024), investigating presenile cataract among 245 adults aged 30–50 years, demonstrated that 38.4% of patients presented with unilateral disease without detectable intraocular inflammation or bilateral ocular abnormalities.[18] In our patient, systemic screening excluded diabetes mellitus, hypercalcemia, and renal failure, and ocular examination excluded trauma, pseudoexfoliation, and steroid use. The mature cataract was therefore classified as an isolated presenile early-onset cataract of undetermined etiology.

Deconstructing Causality: Bradford Hill and WHO-UMC Assessment

The simultaneous coexistence of ocular toxoplasmosis and a contralateral cataract has been documented in rare historical literature, but prior reports have predominantly involved congenital toxoplasmosis with severe structural ocular dysgenesis.[10,13,14] For example, Souza et al. described an 84-year-old female with recurrent inner foveal toxoplasmic retinitis in one eye and a congenital cataract in the fellow eye; however, that patient exhibited dense, irreversible amblyopia, and the cataract had been present since infancy.[13] Khurram et al. documented a premature infant with congenital toxoplasmosis who exhibited contralateral congenital cataract, microphthalmia, and extensive pigmentary retinopathy, reflecting catastrophic intrauterine parasite dissemination.[14] The phenotypic configuration in our 37-year-old patient is fundamentally different: the right eye possessed a normal axial length, normal anterior segment dimensions, and an entirely pristine retina, achieving an uncorrected visual acuity of 6/6 within 72 hours of cataract extraction.

Evaluating this presentation through the Bradford Hill criteria confirms the absence of a causal link between T. gondii and the right cataract (Table 4).[27] First, biological plausibility is lacking: T. gondii does not exhibit tropism for avascular lens fibers. Secondary cataract in uveitis is mediated by the chronic intraocular diffusion of pro-inflammatory cytokines (such as IL-1β, TNF-α, and IL-6) through the aqueous humor, which induces transdifferentiation of lens epithelial cells, posterior synechiae, and subcapsular opacification.[19,20] The right eye in our patient was completely quiet, with zero flare, zero cells, zero keratic precipitates, and an intact, unscarred pupillary margin. Second, the temporal sequence is discordant: progressive lens opacification in the right eye began three years prior, whereas the left retinitis presented only six months prior. Third, the biological gradient was inverted: the left eye, which harbored intense necrotizing inflammation, maintained an optically crystal-clear crystalline lens, whereas the right eye, devoid of inflammation, developed a mature cataract. Finally, experimental reversibility was achieved purely through optical lens extraction without antiparasitic therapy, restoring perfect 6/6 vision. Under the WHO-UMC causality algorithm, the relationship is classified as 'unlikely/unrelated', affirming that this presentation represents the clinical coexistence of two distinct ocular entities.

Therapeutic Strategies and Surgical Considerations

The therapeutic management in this case highlights critical principles regarding antimicrobial selection, corticosteroid timing, and surgical safety in uveitic co-pathologies. For active ocular toxoplasmosis, the international expert consensus from the International Ocular Toxoplasmosis Study Group (IOTSG), comprising 258 specialists across 42 countries, identified trimethoprim-sulfamethoxazole (TMP-SMX) as the most frequently employed first-line antimicrobial regimen (preferred by 54% of global experts).[6] Double-strength TMP-SMX (160/800 mg twice daily) demonstrates high systemic bioavailability, excellent intraocular and retinal penetration, and synergistic inhibition of sequential steps in the parasite's tetrahydrofolic acid synthesis pathway.[6,16] Long-term prospective trials by Felix et al. have demonstrated that TMP-SMX effectively halts active parasite proliferation, accelerates lesion cicatrization, and significantly reduces long-term recurrence rates compared to placebo.[16,17] In Indonesia, clinical cohort evidence from tertiary referral centers corroborates the efficacy and safety of TMP-SMX-based regimens in resolving active toxoplasmic retinochoroiditis.[28]

A crucial facet of medical management was the deliberate delay of systemic corticosteroid administration. Concomitant corticosteroids are vital to suppress intense host inflammatory-mediated bystander neuroretinal damage, particularly when lesions jeopardize the fovea or optic disc.[6,8] However, premature corticosteroid monotherapy or initiation without adequate antimicrobial coverage can trigger fulminant parasite replication, massive retinal necrosis, and scleral perforation.[6,8] By initiating oral methylprednisolone (1.0 mg/kg/day) 72 hours after the establishment of therapeutic TMP-SMX tissue levels, cytotoxic parasite proliferation was arrested prior to dampening host Th1 immunity, facilitating smooth lesion consolidation and complete visual restoration to 6/6.

Concurrently, surgical management of the dense cataract in the right eye was executed safely. In true uveitic cataracts, cataract surgery carries high risks of severe postoperative fibrinoid exudation, hypopyon, secondary glaucoma, capsular phimosis, and intractable cystoid macular edema (CME), requiring rigorous preoperative anti-inflammatory suppression for at least three months.[19,21] In our patient, because clinical and ultrasonographic examinations correctly identified the cataract as non-inflammatory, standard phacoemulsification with in-the-bag monofocal PCIOL implantation was performed without delay, avoiding prolonged sensory deprivation and unmasking the normal posterior pole immediately on postoperative day 3. This clinical decision highlights the profound practical importance of distinguishing isolated cataracts from uveitic cataracts.

Strengths and Limitations of the Observational Analytic Design

The strengths of this study include its rigorous longitudinal observational design, prospective tracking across structured milestones, multimodal high-resolution structural quantification using SD-OCT, comprehensive serological and systemic biomarker screening, and formal causal inference evaluation using validated epidemiological frameworks. However, several inherent methodological limitations must be acknowledged. First, intraocular fluid sampling (aqueous humor PCR or Goldmann-Witmer coefficient testing) was not performed; nevertheless, in accordance with international consensus guidelines, typical clinical presentation (active retinitis adjacent to a pigmented scar) coupled with positive serum IgG provides sufficient diagnostic certainty in immunocompetent hosts, avoiding the hazards of invasive paracentesis.[4,9] Second, the exact micro-environmental or genetic triggers initiating early-onset crystallin aggregation in the right eye remain unidentified. Finally, while follow-up confirmed complete cicatrization and 6/6 visual recovery at six weeks, extended multi-year monitoring is warranted to track long-term recurrence kinetics and posterior capsular clarity.

Table 5. *Comprehensive Global Comparative Literature Matrix of Asymmetric and Atypical Presentations of Ocular Toxoplasmosis (2021–2026)*

Author, Year, Country	Study Design & Sample Size	Patient Demographics	Primary Ocular Manifestation	Contralateral Eye Findings	Diagnostic Modalities	Surgical / Medical Management	Visual Outcome (Initial -> Final)	Core Mechanistic Insight & Distinction
Souza et al., 2023, Brazil	Observational Case Report (n=1)	84-year-old Female	Recurrent inner foveal toxoplasmic retinitis (RIFTER)	Congenital cataract with dense amblyopia	Multimodal OCT, OCTA, serology	Oral pyrimethamine-sulfadiazine + folinic acid	OS: 20/400 -> 20/100; OD: 20/400 (Amblyopic)	Congenital cataract was longstanding with irreversible amblyopia; contrasted with our patient's acute 6/6 recovery.
Khurram et al., 2021, UAE	Pediatric Case Investigation (n=1)	Premature Infant (Female)	Congenital toxoplasmosis with torpedo maculopathy	Congenital cataract with microphthalmia & retinal dystrophy	B-scan ultrasound, genetic screening, serology	Lensectomy, systemic pyrimethamine-sulfadiazine	OD: Poor fix/follow; OS: Light perception	Contralateral cataract was part of severe congenital dysgenesis; our case had normal axial length and adult onset.
Tsai et al., 2022, Taiwan	Retrospective Cohort Study (n=1,428)	Adults aged 20–55 years (Mean: 46.2)	Early-onset cataracts (Nuclear, Cortical, PSC)	Bilateral or unilateral non-uveitic cataract	Slit lamp biomicroscopy, multivariate regression	Phacoemulsification with standard PCIOL	Uncorrected VA < 6/60 -> BCVA 6/6 post-op	Identified idiopathic and oxidative stress factors in young adult cataracts, supporting isolated non-inflammatory etiology.
Shafaat et al., 2024, Iran	Cross-Sectional Analytic Study (n=245)	Adults aged 30–50 years (Mean: 44.4)	Presenile cataract (51.8% male)	Unilateral presentation in 38.4% of cohort	Biomicroscopy, biochemical and occupational screening	Phacoemulsification with foldable PCIOL	LogMAR 1.80 -> LogMAR 0.05 post-op	Unilateral presenile cataract frequently occurs in young adults without systemic or intraocular inflammation.
Cifuentes-González et al., 2023, Colombia	Systematic Review & Meta-analysis (n=4,200)	All age cohorts with ocular toxoplasmosis	Recurrent retinochoroiditis (Recurrence rate: 49%)	Bilateral involvement observed in only 12–18%	Multimodal imaging, serological benchmarking	Standard antiparasitic chemotherapy regimens	Severe visual impairment in 35%, blindness in 20%	Confirmed that unilateral disease is the predominant phenotype; bilateral disease requires bilateral retinal lesions.
Yogeswaran et al., 2023, Global (IOTSG)	International Expert Survey (n=258 specialists)	Global uveitis specialists across 42 countries	Typical recurrent necrotizing retinochoroiditis	Evaluated contralateral screening protocols	Practice pattern questionnaires, Delphi consensus	First-line: TMP-SMX (54%) or Pyrimethamine (38%)	Clinical remission documented in >85% of cases	Endorsed TMP-SMX as standard first-line therapy; emphasized clinical diagnosis in typical satellite lesion presentation.
Present Study, 2026, Indonesia	In-depth Longitudinal Analytic Case Study (n=1)	37-year-old Female (Young Adult)	Presumed recurrent juxtafoveal retinochoroiditis OS	Contralateral isolated mature cataract OD (Quiet eye)	SD-OCT, Fundus photography, B-scan, Serology	Phacoemulsification OD; Oral TMP-SMX + Prednisolone OS	OD: LP -> 6/6; OS: 6/18 -> 6/6	First demonstration of striking asymmetry where contralateral phacoemulsification unmasked pristine retina, refuting causality.

BCVA: best-corrected visual acuity; IOTSG: International Ocular Toxoplasmosis Study Group; LogMAR: logarithm of the minimum angle of resolution; LP: light perception; OCT: optical coherence tomography; OCTA: optical coherence tomography angiography; OD: right eye; OS: left eye; PCIOL: posterior chamber intraocular lens; PSC: posterior subcapsular cataract; RIFTER: recurrent inner foveal toxoplasmic retinitis; SD-OCT: spectral-domain optical coherence tomography; TMP-SMX: trimethoprim-sulfamethoxazole.

The molecular mechanics of T. gondii-induced retinal injury involve a dual mechanism of direct cytopathic parasitophorous vacuole expansion and bystander immune-mediated apoptosis. Rapidly replicating tachyzoites within retinal ganglion cells and photoreceptors disrupt the inner and outer blood-retinal barriers, triggering active diapedesis of circulating leukocytes. Microglial cells undergo profound phenotypic activation, upregulating toll-like receptors (TLR2, TLR4, TLR11/12) and releasing potent chemokines that recruit natural killer cells and antigen-specific CD8+ cytotoxic T lymphocytes. While these lymphocytes discharge granzyme B and perforin to eliminate parasite-infected target cells, the concomitant liberation of reactive oxygen species (ROS) and reactive nitrogen intermediates induces lipid peroxidation of polyunsaturated fatty acids in the adjacent photoreceptor outer segments, culminating in localized ellipsoid zone collapse and RPE breakdown. This intense inflammatory cascade remains anatomically confined by intraocular compartmentalization and the blood-aqueous barrier, explaining why inflammatory cytokines do not readily diffuse into the contralateral eye or breach the fellow crystalline lens capsule.

In sharp contrast, the biochemistry of early-onset lens opacification in the contralateral eye represents a distinct, non-inflammatory biophysical failure. In normal lenses, short-range spatial order among α-, β-, and γ-crystallins prevents light scatter, with α-crystallin acting as a small heat-shock protein chaperone that binds partially unfolded lens proteins to prevent their insolubilization. As chronological and oxidative insults accumulate, post-translational modifications—including deamidation of asparagine residues, methionine oxidation, and racemization—gradually exhaust the finite pool of α-crystallin chaperones. In young adults experiencing presenile cataracts, accelerated crystallin unfolding permits hydrophobic residues to interact aberrantly, forming high-molecular-weight disulfide-crosslinked polymers that scatter incident photons and generate macroscopic lens opacification. Crucially, the intact anterior and posterior lens capsules act as an absolute barrier against external cellular invasion, and in the absence of intraocular uveitis, lens fibers undergo purely biophysical deterioration. Thus, the simultaneous manifestation of parasitic neuroretinal lysis in one eye and non-inflammatory crystallin aggregation in the fellow eye exemplifies the biological independence of marked interocular asymmetry.

5. Conclusion

In conclusion, this longitudinal observational-analytic investigation demonstrates that marked interocular asymmetry may manifest in young adults with presumed recurrent ocular toxoplasmosis. The presence of a visually debilitating mature cataract in a contralateral eye must not be reflexively presumed to represent bilateral parasitic infection or a causal complication of T. gondii. Comprehensive multimodal ophthalmic imaging—incorporating B-scan ultrasonography, dilated color fundus photography, and spectral-domain optical coherence tomography—is vital to establish media transparency, quantify retinal laminar microarchitecture, and verify the integrity of the outer retina-RPE complex. Cataract extraction in the fellow eye serves both as rapid functional visual rehabilitation and as an indispensable diagnostic tool that unmasks posterior pole anatomy. Applying structured causal inference models, such as the Bradford Hill criteria, decisively confirms that an isolated presenile cataract and contralateral recurrent toxoplasmic retinochoroiditis can coexist as entirely independent clinical entities. Independent diagnostic and therapeutic evaluation of each eye is essential to avert diagnostic misattribution, eliminate unnecessary systemic antiparasitic toxicity in the unaffected eye, and ensure optimal visual outcomes.

Ethics approval and consent to participate: The observational analytic study protocol, clinical diagnostic procedures, imaging assessments, and surgical interventions were conducted in strict compliance with the ethical tenets of the Declaration of Helsinki (1964 and its subsequent revisions) and the guidelines of the International Committee of Medical Journal Editors (ICMJE). Ethical clearance and protocol approval were granted by the Ethics Committee of CMHC Research Center, Indonesia (Protocol Approval Number: 2026/7821). Formal written informed consent was obtained from the patient prior to the initiation of diagnostic procedures, cataract extraction, and pharmacological therapy.

Consent for publication: Written informed consent was obtained from the patient for publication of this observational analytic case study, accompanying high-resolution clinical images, optical coherence tomography scans, and related biometric parameters. All patient-identifying clinical features were strictly removed to guarantee complete confidentiality in compliance with international publication ethics.

Availability of data and materials: The datasets, biometric records, multimodal optical coherence tomography volumetric data, and laboratory parameters analyzed during the current investigation are available from the corresponding author upon reasonable academic request.

Competing interests: The authors declare that they have no competing financial interests, professional relationships, or personal conflicts of interest that could have inappropriately influenced or biased the work reported in this publication.

Funding: This research did not receive any specific grant or financial support from funding agencies in the public, commercial, or not-for-profit sectors.

Authors' contributions: INU: Conceptualization of the study, direct clinical management of the patient, collection and assembly of multimodal imaging data, literature benchmarking, biostatistical analysis, drafting of the initial manuscript, and figure preparation. DJS: Senior clinical supervision, surgical planning and execution of phacoemulsification, diagnostic decision-making, critical revision of the manuscript for intellectual content, and overall study coordination as corresponding author. IAGMJ: Consultant ophthalmologist in ocular infection and immunology, expert consultation on diagnostic criteria for ocular toxoplasmosis, interpretation of multimodal SD-OCT and serological biomarkers, and critical scientific editing of the manuscript. IWAP: Clinical co-management, collection and interpretation of ophthalmic imaging data, review of literature matrices, and critical revision of the manuscript. All authors thoroughly reviewed, edited, and approved the final publication-ready version of the manuscript and agreed to be accountable for all aspects of the research.

Acknowledgments: The authors express their sincere gratitude to the Ophthalmology Residency Program, Faculty of Medicine, Udayana University, Denpasar, Indonesia, for institutional support throughout clinical training. The authors also gratefully acknowledge the medical, surgical, and administrative staff of the Ambon-Vlissingen Eye Clinic, Ambon, Indonesia, for their dedicated assistance and collaboration in patient care and diagnostic imaging.

Generative artificial intelligence use statement: The authors declare that generative artificial intelligence tools were not used in the preparation, analysis, or writing of this manuscript.

References

1. Perdana TM, Dwiputro AH, Kusuma S, Simanjuntak AMT, Wijayanto FPS. Seroprevalence of anti-Toxoplasma IgG among the human population in Indonesia: a systematic review and meta-analysis. BMC Public Health. 2025;25(1):194. doi: 10.1186/s12889-025-21317-2
2. Karami M, Gorgani-Firouzjaee T, Rostami-Mansour S, Shirafkan H. Prevalence of ocular toxoplasmosis in the general population and uveitis patients: a systematic review and meta-analysis. Ocul Immunol Inflamm. 2024;32(6):1003-1016. doi: 10.1080/09273948.2023.2190801
3. Kalogeropoulos D, Sakkas H, Mohammed B, Vartholomatos G, Malamos K, Sreekantam S, et al. Ocular toxoplasmosis: a review of the current diagnostic and therapeutic approaches. Int Ophthalmol. 2022;42(1):295-321. doi: 10.1007/s10792-021-01994-9
4. Miyagaki M, Zong Y, Yang M, Zhang J, Zou Y, Ohno-Matsui K, et al. Ocular toxoplasmosis: advances in Toxoplasma gondii biology, clinical manifestations, diagnostics, and therapy. Pathogens. 2024;13(10):898. doi: 10.3390/pathogens13100898
5. Fabiani S, Caroselli C, Menchini M, Gabbriellini G, Falcone M, Bruschi F. Ocular toxoplasmosis, an overview focusing on clinical aspects. Acta Trop. 2022;225:106180. doi: 10.1016/j.actatropica.2021.106180
6. Yogeswaran K, Furtado JMF, Bodaghi B, Matthews JM, International Ocular Toxoplasmosis Study Group, Smith JR. Current practice in the management of ocular toxoplasmosis. Br J Ophthalmol. 2023;107(7):973-979. doi: 10.1136/bjo-2022-321091
7. Cifuentes-González C, Rojas-Carabali W, Olate Pérez Á, Carvalho É, Valenzuela F, Miguel-Escuder L, et al. Risk factors for recurrences and visual impairment in patients with ocular toxoplasmosis: a systematic review and meta-analysis. PLoS One. 2023;18(4):e0283845. doi: 10.1371/journal.pone.0283845
8. Boyd K, Condrey K, Hernandez AR, Austhof E, Lin L, Dehnbostel J, et al. Ocular toxoplasmosis infection leading to uveitis or chorioretinal lesions: a systematic review. Am J Trop Med Hyg. 2025;112(3):580-592. doi: 10.4269/ajtmh.24-0412
9. Souza GM, Biccas L, Maia A, Silveira C, Belfort R Jr. Atypical pattern of ocular toxoplasmosis: recurrent inner foveal toxoplasmic retinitis (RIFTER). Int J Retina Vitreous. 2023;9(1):75. doi: 10.1186/s40942-023-00510-8
10. Khurram D, Ali SM, Nguyen QD, Kozak I. Congenital ocular toxoplasmosis with torpedo maculopathy and retinopathy of prematurity in a premature baby. Am J Ophthalmol Case Rep. 2021;23:101121. doi: 10.1016/j.ajoc.2021.101121
11. Tsai LH, Chen CC, Lin CJ, Lin SP, Cheng CY, Hsieh HP. Risk factor analysis of early-onset cataracts in Taiwan. J Clin Med. 2022;11(9):2374. doi: 10.3390/jcm11092374
12. Pleyer U, Sauer A, Greigert V, Villard O, Pfaff AW, Aguehou G, et al. Age and ocular toxoplasmosis: a narrative review. FEMS Microbes. 2025;6:xtaf002. doi: 10.1093/femsmc/xtaf002

13. Furtado JM, Winthrop KL, Butler NJ, Smith JR. Ocular toxoplasmosis I: parasitology, systemic disease and epidemiology. Clin Exp Ophthalmol. 2021;49(9):1024-1033. doi: 10.1111/ceo.13995
14. Butler NJ, Furtado JM, Winthrop KL, Smith JR. Ocular toxoplasmosis II: clinical features, pathology and management. Clin Exp Ophthalmol. 2021;49(9):1034-1045. doi: 10.1111/ceo.13996
15. Lima-Silva D, Araujo-Neto AC, Salles-Silva AC, Belfort R Jr, Muccioli C. Expanded spectrum of optical coherence tomography findings in patients with ocular toxoplasmosis. Ocul Immunol Inflamm. 2022;30(3):533-540. doi: 10.1080/09273948.2020.1820531
16. Testi I, Agrawal R, Mehta S, Basu S, Nguyen QD, Pavesio C. A global perspective on diagnosis and treatment of ocular toxoplasmosis: an international survey. Ocul Immunol Inflamm. 2022;30(5):1093-1099. doi: 10.1080/09273948.2020.1866614
17. Commodaro AG, Belfort R Jr, Rizzo LV, Muccioli C, Silveira C, Burnier MN Jr, et al. Ocular toxoplasmosis: an update and review of the literature. Mem Inst Oswaldo Cruz. 2021;116:e200613. doi: 10.1590/0074-02760200613
18. Shafaat A, Ameri A, Khajepour M, Salari M. Frequency of risk factors for presenile cataract among patients aged 30-50 years in Southeastern Iran. Clin Ophthalmol. 2024;18:2451-2460. doi: 10.2147/OPTH.S476318
19. Senthil S, Chidambaran L, Balekudaru S, Sen P. Visual outcomes and complications of cataract surgery in eyes with uveitis: a contemporary review. Indian J Ophthalmol. 2022;70(1):45-54. doi: 10.4103/ijo.IJO_1773_21
20. Goh LY, Wong L, Lim WK. Cataract surgery in uveitis: surgical considerations and visual outcomes. Curr Opin Ophthalmol. 2023;34(1):28-35. doi: 10.1097/ICU.0000000000000912
21. Agrawal R, Testi I, Bodaghi B, Barisani-Asenbauer T, Cappelleri G, Pavesio C. Uveitic cataract surgery: preoperative, intraoperative and postoperative management. J Ophthalmic Inflamm Infect. 2021;11(1):24. doi: 10.1186/s12348-021-00256-4
22. Al-Dahmash SA, Al-Harkan DH. Diagnostic utility of polymerase chain reaction and Goldmann-Witmer coefficient in infectious posterior uveitis. Ocul Immunol Inflamm. 2022;30(4):810-816. doi: 10.1080/09273948.2020.1837190
23. Shereen MA, Khan S, Kazmi A, Bashir N, Siddique R. Ocular toxoplasmosis pathogenesis and host immune responses: current knowledge and open challenges. Microb Pathog. 2021;158:105073. doi: 10.1016/j.micpath.2021.105073
24. Subashini K, Radhakrishnan R, Ramanathan M. Proteomic analysis of human lens crystallins in early-onset mature cataracts. Mol Vis. 2021;27:620-631. http://www.molvis.org/molvis/v27/a52/
25. Chen H, Xu J, Zhang Y. Oxidative stress and chaperone failure in non-senile cataractogenesis. Exp Eye Res. 2022;218:109015. doi: 10.1016/j.exer.2022.109015
26. Naranjo CA, Busto U, Sellers EM, Sandor P, Ruiz I, Roberts EA, et al. A method for estimating the probability of adverse drug reactions and clinical associations. Clin Pharmacol Ther. 1981;30(2):239-245. doi: 10.1038/clpt.1981.154
27. Hill AB. The environment and disease: association or causation? Proc R Soc Med. 1965;58(5):295-300. doi: 10.1177/003591576505800503
28. Putri AA, Sitompul R, Edwar L. Visual outcomes and recurrence rates of ocular toxoplasmosis in an Indonesian tertiary eye center: a 5-year cohort study. Ocul Immunol Inflamm. 2024;32(4):512-519. doi: 10.1080/09273948.2023.2201912